Order at the boundaries of phase-shifted 7×7 domains on Si(111)

1996 J. Phys.: Condens. Matter 8 8743

(http://iopscience.iop.org/0953-8984/8/45/010)

J. Phys.: Condens. Matter **8** (1996) 8743–8751. Printed in the UK

Order at the boundaries of phase-shifted 7×7 domains on Si(111)

M T Cuberes and J L Sacedón

Instituto de Ciencia de Materiales de Madrid (CSIC), Cantoblanco, E-28049 Madrid, Spain

Received 17 May 1996, in final form 25 July 1996

Abstract. We report the observation by means of a scanning tunnelling microscope (STM) of phase-shifted 7×7 domains on Si(111) linked by order compatible with a $(7/\sqrt{3} \times 7/\sqrt{3})$ R 30° reconstruction. Such structure was obtained by annealing an Sb film 30 ML thick deposited at room temperature on the virgin Si(111) 7×7 surface. The voltage-dependent STM features of the reconstruction found at the 7×7 domain boundaries can be explained by a dislocation-based structural model that assumes the presence of Sb. The model can account for the matching of the 7×7 domains and passivates the boundary regions completely.

1. Introduction

Phase-shifted 7×7 domains are commonly observed on Si(111) surfaces [1–18]. The domain boundary regions, often called 'out-of-phase boundaries' (OPBs) constitute a 2D defect which affects epitaxial growth. OPBs may affect the step configuration on Si surfaces [3, 4], induce the formation of metastable reconstructions in Si homoepitaxial growth [5], or act as preferential nucleation sites in molecular beam epitaxy (MBE) on Si(111) [6].

The mechanisms that cause the formation of distinct domains and the factors that influence the number and distribution of OPBs are subjects of current research. The basic explanation for the presence of different domains is that they form during the 1×1 to 7×7 transition on Si(111). As this is a first-order transition, it proceeds by the nucleation of 7×7 islands which form OPBs as they coalesce. The kinetics of steps and domain structures during the phase transition have been studied by low-energy electron microscopy (LEEM) [7–10], reflection electron microscopy (REM) [11–13], secondary-electron imaging (SEM) [14] and STM [15–17]. The density of domain boundaries can be altered by annealing below the 1×1 to 7×7 transition temperatures [14, 18]. The presence of impurity atoms, or an excess of dopants can also alter the OPBs density.

In this work we report the observation by means of the STM of phase-shifted 7×7 domains on the Si(111) surface *linked by order* compatible with a $(7/\sqrt{3} \times 7/\sqrt{3})$ R 30° reconstruction in the domain boundary region. Since this structure was obtained by annealing the surface initially covered with an Sb film 30 ML thick (see the experiment) we infer that the presence of Sb atoms increased the number of distinct 7×7 domains nucleated during the 1×1 to 7×7 phase transition and that Sb is also involved in the reconstruction found at the boundaries.

We posed ourselves the question of whether the coexistence of phase-shifted 7×7 domains could in some cases be related to bulk dislocations emerging to the surface in the domain boundary regions. In particular, in our experiment Sb atoms inhomogeneously

0953-8984/96/458743+09$19.50

located at substitutional sites during the annealing stage could provide enough stress to nucleate dislocations at a (111) bulk near-surface plane, due to the different sizes of the Sb and Si atoms (covalent radii of Sb = 1.45 Å, and of Si = 1.17 Å). In a more general case, the activation of gettering mechanisms when annealing in the presence of impurities may lead to an increase of the dislocation density next to the surface.

In principle, from a measurement of the phase-shift between the distinct 7×7 domains it should be possible to decide whether a bulk dislocation is emerging at the boundary. However, STM measurements do not usually allow enough precision to distinguish whether this is the case due to creep and non-linearity of the piezoelectric elements. The possibility that a bulk dislocation terminating at the surface is responsible for the presence of phase-shifted domains on the Si(111) 7×7 surface is usually overlooked in STM studies of OPBs [19].

Nevertheless, in our case, assuming that Sb occupies certain substitutional sites, we propose and discuss a structural model which (i) can account for the voltage-dependent STM images of the reconstruction found at the domain boundaries, (ii) can explain the matching of the Si(111) 7×7 domains, and (iii) can completely passivate the domain boundary region even if emerging bulk dislocations are present.

2. Experiment

The sample preparation and STM measurements were performed in ultra-high vacuum (UHV) at a base pressure of 5×10^{-11} mbar, using a commercial OMICROM-STM. The Si (111) sample was carefully cut from an n-type P-doped ($\rho = 0.1$–$5\ \Omega\ \mathrm{cm}^2$) Si(111) wafer (AUREL-WACKER), directly introduced into the vacuum chamber and degassed at 700 °C for ≈12 hours before carrying out the usual thermal procedures to obtain a 7×7 reconstruction. On the virgin Si(111) 7×7 surface STM topographies of dimensions 3000 Å × 3000 Å always showed a single 7×7 domain and no traces of anomalous contamination or defects. The surface structure that we are concerned with in this work was obtained after room temperature deposition of an Sb overlayer 30 ML (1 ML Sb ≡ 2.8 Å) thick on the Si(111) 7×7 surface [20] and subsequent annealing. Sb was evaporated by means of a Knudsen cell at a rate of ≈0.5 ML min^{-1} calibrated with a quartz crystal microbalance. The thermal treatment carried out on the 30 ML Sb/Si(111) 7×7 interface was the same as that on the virgin Si(111) to obtain the 7×7 reconstruction, namely (i) heating the interface up to 1200 °C for 2 min in UHV conditions (in the 10^{-9} mbar range), (ii) rapid cooling down to 900 °C, and holding at this temperature for 10 min, and (iii) slow cooling at a rate of ≈1 °C s^{-1} down to room temperature. This annealing procedure is the one commonly used to obtain good quality Si(111) 7×7 surfaces with a new Si(111) sample, typically covered by a native oxide layer.

3. Results and discussion

3.1. Reconstruction linking phase-shifted 7×7 *domains*

Figures 1(a) and 1(b) show STM images of the treated surface taken after deposition and annealing with a sample voltage of $V_s = 2$ V and a tunnelling current of $I = 1.6$ nA. The presence of different 7×7 domains linked by order in the boundary region is apparent.

In figures 1(a) and 1(b) the lines MN and OP have been traced to indicate the phase-shift between the 7×7 units. Although the image does not provide enough precision, the 7×7 cells can be considered displaced by $\frac{1}{6}d$ or $\frac{1}{3}d$ ($d \equiv$ the long diagonal of the 7×7 unit

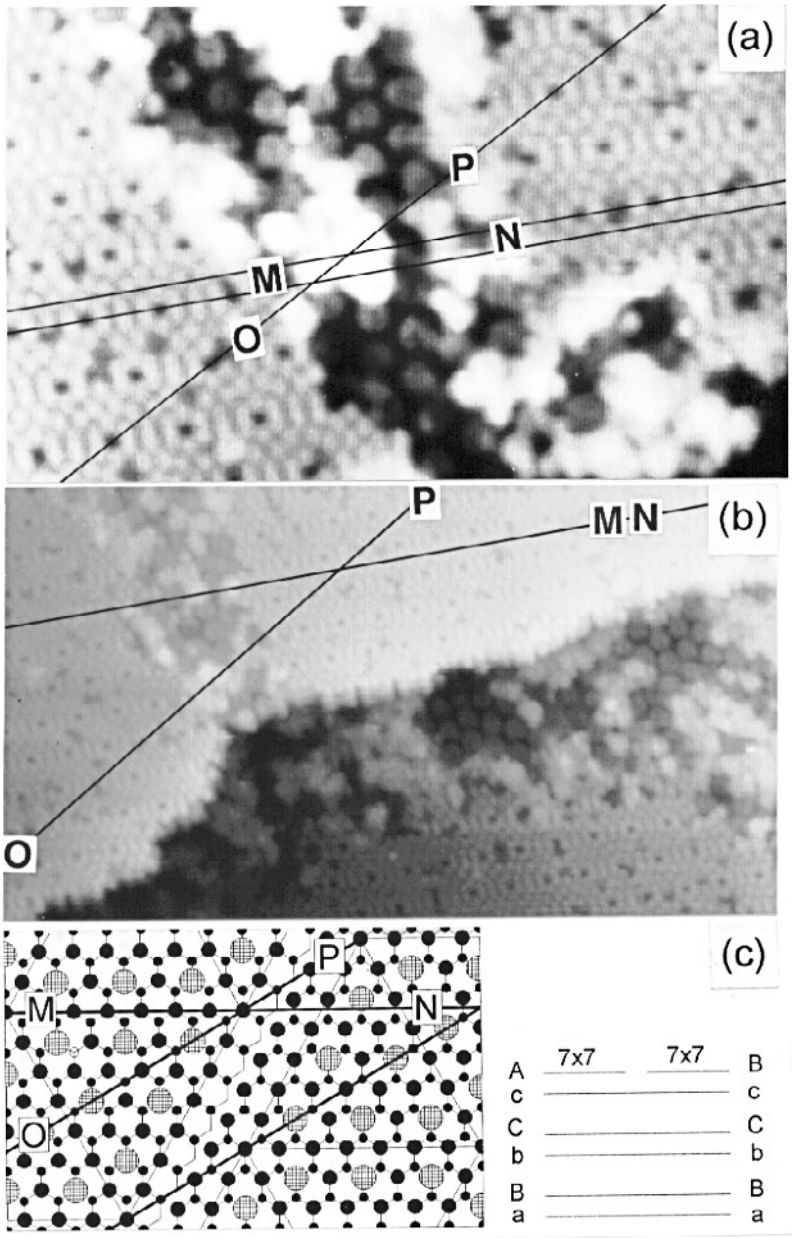

Figure 1. (a), (b) STM images taken with $V_s = 2$ V, $I = 1.6$ nA on a thermally treated Sb/Si(111) surface. The phase-shift between the 7×7 domains can be measured following the lines MN and OP, and it is compatible with the presence of a dislocation emerging from the bulk at the domain boundary. A new reconstruction is found in the domain boundary regions. (c) Adatoms of the 7×7 reconstruction on the last bilayer of the ideal bulk-like termination of the (111) surface. Two 7×7 domains are drawn with a phase-shift compatible with the experimental data.

cell) along the direction of d (i.e. the direction normal to MN). Then the last Si substrate layer below the three layers that form the 7×7 reconstruction [21] would have a different

stacking for each domain, in such a way that at least a 30° partial dislocation [22] runs along a ⟨110⟩ direction in a (111) plane parallel to the surface. This is illustrated in figure 1(c), where the atoms of the last bilayer of the ideal bulk-like termination of the (111) surface and the adatoms of the 7×7 units have been drawn. The same atomic geometry at the surface is obtained if the dislocation is introduced at the last non-reconstructed substrate bilayer (as drawn in figure 1(c)) or at a deeper bilayer. In this respect, some additional information is given by STM images taken at a negative sample voltage. Since in our case the orientation of the faulted and unfaulted triangular halves of the 7×7 unit is the same for both domains (the images are not shown here), the dislocation(s) should lie at a bilayer below the last non-reconstructed one.

In figure 1(b) the two 7×7 domains coexist at the upper-step terrace while on the lower terrace only one 7×7 domain is present. The height of the step in figure 1(b) is the usual value for single-domain Si(111) 7×7 surfaces (≈3.1 Å). An adequate arrangement of the phase-shifts between the 7×7 units at the upper- and lower-step terraces could also lead to the conclusion (compatible with the STM data) that a dislocation line running along the step is present in the substrate.

Besides the 7×7 reconstruction, order is found at the boundary of the 7×7 domains. It is noticeable from figures 1(a) and 1(b) that the regions with the new structure lie somewhat (≈0.7 Å) deeper than the 7×7 domain terraces. The structure appears in the empty-state images as formed by rings ≈16 Å apart from centre to centre, aligned along crystallographic directions rotated by 30° relative to those that define the 7×7 cell. Although order is apparent in the regions with the new reconstruction, they are in general defective. Some disordered atoms grouped at places lying above these regions are also seen in both images.

Ring-like structures rather similar to those that appear in figures 1(a) and 1(b) have been observed in empty-state STM images from Si(111) surfaces upon Ni deposition [23]. Co and/or other transition metal contaminants are also known to induce ring-like features on Si(111) giving rise to the formation of an 'impurity-stabilized 1×1' surface [24], with impurity-induced rings that appear randomly distributed. These superstructures were formed after deposition of the transition metal contaminants on the Si(111) surface. Here we discuss the interrelation of an ordered array of rings with 7×7 domain boundaries that we have reproducibly observed when annealing in the presence of an Sb layer. We have not observed this structure when performing exactly the same thermal treatment on a virgin Si(111) surface (in the absence of Sb), and therefore we find unlikely that in our case the ring-like features are induced by transition metal contaminants. Although the STM does not allow an unequivocal identification of the chemical elements on the surface, the structural model discussed in the next section is based in the presence of Sb in the domain boundary regions.

3.2. The structural model

Figure 2 illustrates our model for explaining the order observed at the domain boundary, assuming the presence of dislocations emerging from the bulk in the region. We consider a dislocation-based structural model where Sb atoms occupy certain substitutional sites in the 7×7 unit and in the near-surface layers. As can be seen in figure 2, the model can account for the measured phase-shift between the 7×7 domains.

In figure 2 the basis of the new reconstruction is outlined by a hexagon. This hexagon is best understood by placing it at either triangular half of the 7×7 unit as shown at the inset. According to our model, Sb substitutes for the Si rest-atoms, and the Si atoms in the rest-atom layer bonded to the central Si adatoms (marked by triangles). Si rest-atoms

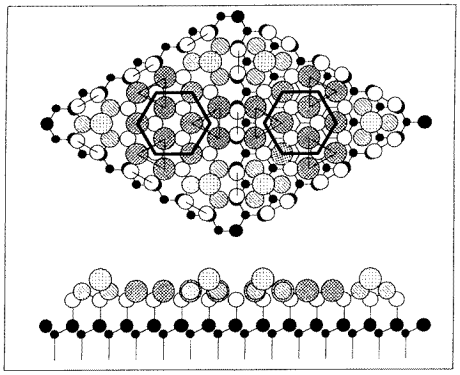

Sb atoms

For passivation along the dislocation lines:

Si (1 db) replaced by Sb

Sb (1db + 1 lp) replaced by Si

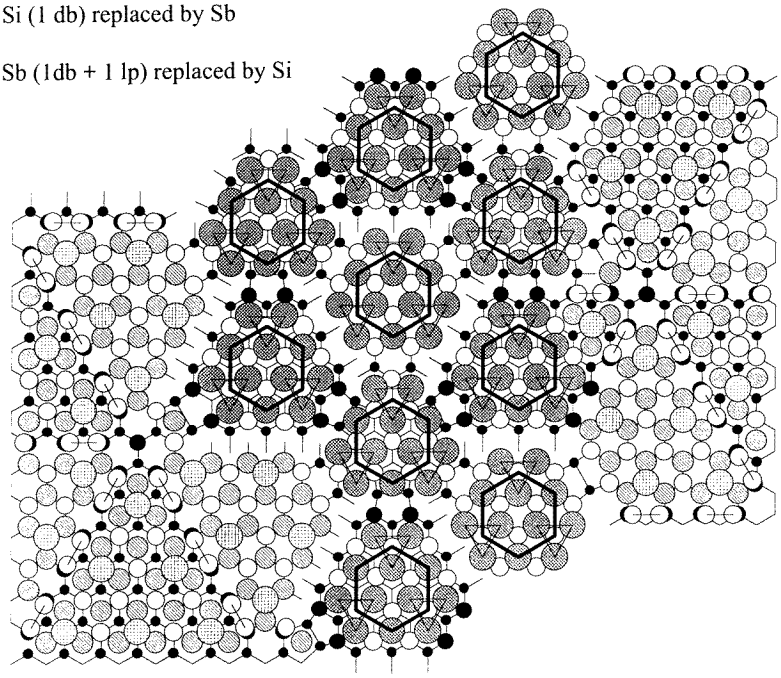

Figure 2. The structural model proposed to explain the order found in the 7×7 domain boundary regions. Two 7×7 domains are drawn at the sides, linked by a $(7/\sqrt{3} \times 7/\sqrt{3})$ R 30° superstructure. By appropriately placing Sb and/or Si atoms and relying on electron-counting arguments, the domain boundary region can be constructed so that there are no half-filled bonds (see the text) (db ≡ dangling bond, lp ≡ lone pair). Inset: the 7×7 unit according to the DAS model [21], without the central Si adatoms. Sb replaces Si in particular sites (see the text).

have a filled hybrid dangling bond and are therefore negatively charged. Sb at a rest-atom position would still have a hybrid lone-pair orbital but would stay neutral. Consequently, the location of Sb at rest-atom sites is expected to be energetically favourable. Sb at these rest-atom positions in the 7×7 unit has been previously suggested on the basis of

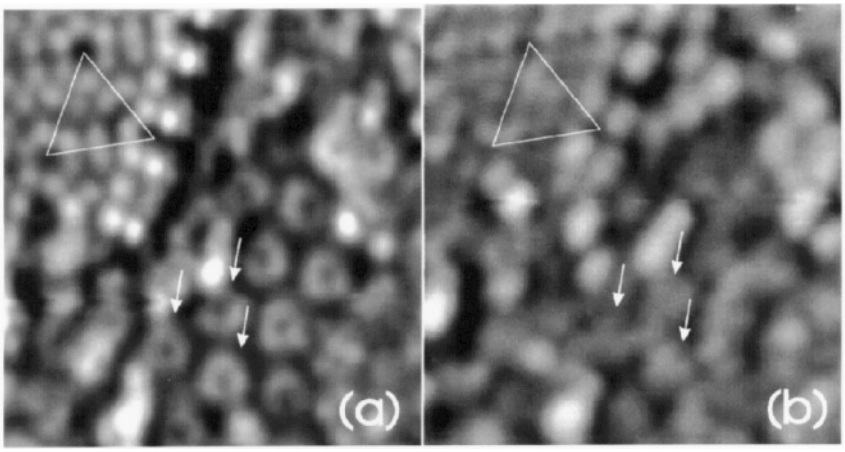

Figure 3. STM images taken with (a) $V_s = 2$ V, $I = 1.6$ nA and (b) $V_s = -2$ V, $I = 2.6$ nA. The arrows are intended as an aid to locating the equivalent reconstructed features for the different voltages.

a scanning tunnelling spectroscopy study [25]. Relying on electron-counting arguments, Sb substitution for Si at the atomic positions in the rest-atom layer marked by triangles in the figure would fill the adatom-related S1 surface band [26]. However, Sb at these sites may not form covalent bonds with the central Si adatoms, but remain with their lone-pair orbitals protruding outside the surface. The Si adatoms no longer covalently bonded to their previous positions would be free to move around and group in the surroundings. According to these assumptions, the disordered atoms lying above the reconstructed region seen in figures 1(a) and 1(b) can be mainly identified as grouped Si adatoms. In addition, Sb in substitutional sites in the rest-atom layer also explains the fact that the regions with the new reconstruction lie deeper than the 7×7 terraces.

The separation of the two hexagons sketched in a 7×7 cell (the inset in figure 2) is in nice agreement with the measured separation of the rings of the new reconstruction. However, with these hexagons on a single 7×7 domain it is not possible to form a hexagonal Bravais net. The order observed in figures 1(a) and 1(b) can be explained by introducing the appropriate 30° partial dislocation lines running along $\langle 110 \rangle$ directions as shown in figure 2. Then, a $(7/\sqrt{3} \times 7/\sqrt{3})$ R 30° reconstruction that accounts for the experimental results is obtained.

We demonstrate now that this reconstruction can passivate completely the domain boundary region. First we discuss the bulk-like layers (the top surface layer will be discussed later): since all of the dislocations in the model run along $\langle 110 \rangle$ directions, Si atoms in the near-surface layers along the dislocation lines may remain with a single or with two dangling bonds. Whenever a Si atom has a single dangling bond (db) pointing towards the dislocation line, Sb can substitute for the corresponding atom, so the dangling bond is replaced with a lone pair (lp) (notice that we are now assuming that Sb also occupies substitutional bulk sites along the dislocation lines in the near-surface region). This process is expected to be energetically favourable since it leads to a reduction of the dangling-bond density. Those Si atoms remaining with two dangling bonds may form dimers parallel to the dislocation line by a slight displacement of their positions in the corresponding layer. Thus, the unsaturated bonds would reside at the top surface layer. Also, the top surface layer in the reconstructed areas is only formed by Sb atoms after the introduction of the dislocations.

Only the hexagons remain in the top surface layer after the introduction of dislocations in the former 7×7 unit in the inset of figure 2. Sb atoms bordering the dislocation lines have one dangling bond and a lone pair. By placing Si instead of Sb at these sites, the two valence Si electrons in the two dangling bonds can fill one bond and leave the other empty. Thus, the reconstructed region can be arranged without any half-filled bond. The total Sb coverage involved in the reconstruction will depend on the depth of the dislocations with respect to the top surface layer. In the top surface layer in the domain boundary regions at least six Sb atoms per former 7×7 unit (giving rise to two ring-like features) are needed for the reconstruction.

3.3. Voltage-dependent STM images

The STM images of the reconstruction at the 7×7 domain boundaries present a strong dependence on the tunnelling voltage. Figure 3 shows two STM images obtained for the same surface region, recorded one immediately after the other, with (a) $V_s = 2$ V, $I = 1.6$ nA and (b) $V_s = -2$ V, $I = 2.6$ nA. A reference for the location of the features in both images is obtained from the position of the 7×7 corner holes in the upper part of the figure. By imaging empty sample states, the rings of figures 1(a) and 1(c) are obtained in figure 3(a). Three threefold-symmetry maxima are distinguished around the ring hole. By imaging filled sample states, for each ring we now find protrusions (see figure 3(b)). The order of the reconstruction cannot be as clearly recognized in the empty-state image as in the filled-state image. Additional protrusions in the image that appear when imaging empty states are probably due to local defects. The voltage dependence of the images is consistent with the model proposed. Tunnelling into the empty Si dangling hybrids or half-filled Sb bonds adjacent to the dislocation lines explains the ring-like features in the empty-state images, while tunnelling to the Sb lone-pair orbitals located at the atomic positions inside the hexagons can give rise to protrusions that account for the filled-state images.

3.4. Large topographic images

The general aspect of this surface with the distinct 7×7 domains linked by the $(7/\sqrt{3} \times 7/\sqrt{3})$ R 30° reconstruction can be grasped from figure 4. The image, taken with $V_s = 2$ V and $I = 1.6$ nA, corresponds to a 2000 Å $\times$ 2000 Å region. Up to four different terraces are found, bordered by steps $\approx$3.1 Å high. Although the registry at each 7×7 domain cannot be measured with enough precision, the symmetric arrangement of domains and steps makes appealing the idea that they are defined by an array of dislocations. Such symmetric arrangements of 7×7 domains and steps have been previously observed in STM measurements [27]. The diagram on the lower left of the figure indicates a possibility for the registry in the different domains, compatible with the STM measurements, in which this would be the case. Provided that the registry of the 7×7 adatom layer could be stated with enough precision to affirm the presence of dislocations, the stacking of the last surface layers along the lines $11'$, $22'$ and $33'$ would be straightforwardly deduced. Then, in our case, the dislocations could lie deeper in the substrate, but not closer to the surface, since the faulted and unfaulted halves of the 7×7 unit cell point in the same direction in the different domains. We always find the new order in the form of a $(7/\sqrt{3} \times 7/\sqrt{3})$ R 30° reconstruction in the domain boundary regions on the same terrace, and next to the lower-step-edge regions, extending right up to the step edge, where according to our model the lower-step surface layer experiences a stacking change.

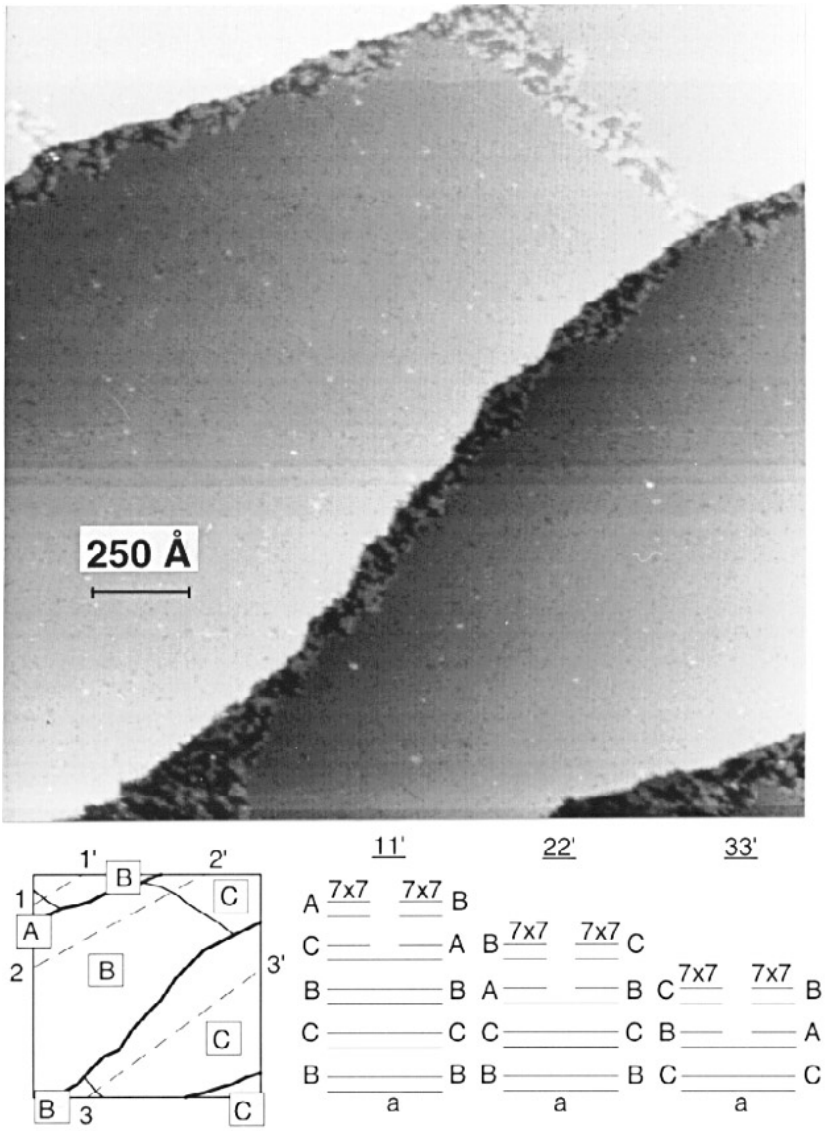

Figure 4. A 2000 Å × 2000 Å STM image taken with $V_s = 2$ V and $I = 1.6$ nA. A drawing with a possible registry at each 7×7 domain (compatible with the STM measurements) is shown lower right. The stacking of the last surface layers along the lines 11′, 22′ and 33′ (dashed in the diagram) according to the said registry is represented on the left.

4. Conclusions

In conclusion, we have presented STM images of a surface structure on Si(111) that consist of phase-shifted 7×7 domains linked by order in the boundary regions. A dislocation-based structural model assuming the presence of Sb has been proposed to explain the voltage-dependent STM features of the reconstruction in the boundary region and account for the phase-shift of the 7×7 domains. Our study points out the often overlooked possibility that

phase-shifted Si(111) 7×7 domains can be related to bulk dislocations emerging to the surface.

Acknowledgments

The authors are indebted to R Saiz-Pardo and F Flores for many discussions on the physics involved in the STM images. C Ocal is gratefully acknowledged for helpful comments on the experimental data. We also thank T Jung for interesting and helpful discussions. This was done under contract number PB-91-930 (DGICT, Spain).

References

[1] Gu Q J, Zhao W B, Ma Y L, Liu N, Xue Y Q and Pang S J 1995 *J. Vac. Sci. Technol.* B **13** 1261
[2] Gu Q J, Ma Z L, Liu N, Ge X, Zhao W B, Pang S J and Hua Y Z 1995 *Surf. Sci.* **327** 241
[3] Tanishiro Y, Takayanagi K and Yagi K 1983 *Ultramicroscopy* **11** 95
[4] Tanaka H, Udagawa M, Itoh M, Uchizama T, Watanabe Y, Yokotsuka T and Sumita I 1992 *Ultramiscroscopy* **42–44** 864
[5] Yang Y-N and Williams E D 1995 *Phys. Rev.* B **51** 13 238
[6] Köhler U, Demuth J E and Hamers R J 1989 *J. Vac. Sci. Technol.* A **7** 2860
[7] Telieps W and Bauer E 1985 *Surf. Sci.* **162** 163
[8] Bauer E, Mundschau M, Swiech W and Telieps W 1991 *J. Vac. Sci. Technol.* A **9** 1007
[9] Paneuf R J, Bartelt N C, Williams E D, Swiech W and Bauer E 1992 *Surf. Sci.* **268** 227
[10] Sakai Y, Kato M, Masuda S, Harada Z and Ichinokawa T 1995 *Surf. Sci.* **336** 295
[11] Osakabe N O, Tanishiro T, Zagi K and Honjo G 1981 *Surf. Sci.* **109** 353
[12] Yamaguchi H and Yagi K 1993 *Surf. Sci.* **287+288** 820
[13] Latyshev A V, Aseev A L, Krasilnikov A B and Stenin S T 1990 *Surf. Sci.* **227** 24
[14] Aizawa N and Homma Y 1995 *Surf. Sci.* **340** 101
[15] Miki K, Morita Y, Tokumoto H, Sato T, Iwatsuki M, Suzuki M and Fukuda T 1992 *Ultramicroscopy* **42-44** 851
[16] Tanaka H, Udagawa T, Itoh M, Uchizama T, Watanabe Z, Zokotsuka T and Sumita I 1992 *Ultramicroscopy* **42+43** 864
[17] Suzuki M, Hibino H, Homma Y, Fukuda T, Sato T, Iwatsuki M, Miki K and Tokumoto H 1993 *Japan. J. Appl. Phys.* **32** 3247
[18] Phaneuf R J, Bartelt N C, Williams E D, Swiech W and Bauer E 1992 *Surf. Sci.* **268** 227
[19] See, e.g.,
Itoh M, Tanaka H, Watanabe Y, Udagawa M and Sumita I 1993 *Phys. Rev.* B **47** 2216 and references therein
[20] STM images taken at different stages of the deposition process revealed morphological changes of the Sb overlayer due to an amorphous–polycrystalline transition in the growth mode; see
Cuberes M T, Ascolani H, Moreno M and Sacedón J L 1996 *J. Vac. Sci. Technol.* B **14** 1665
[21] Takayanagi K, Tanishiro Y, Takahashi M and Takahashi S 1985 *J. Vac. Sci. Technol.* A **3** 1502
[22] Hirth J and Lothe J 1982 *Theory of Dislocations* (New York: Wiley)
[23] Wilson R and Chiang S 1987 *Phys. Rev. Lett.* **58** 2575
[24] Bennett P A, Copel M, Cahill D, Falta J and Tromp R M 1992 *Phys. Rev. Lett.* **69** 1224
[25] Elswijk H B, Dijkkamp D and van Loenen E J 1991 *Phys. Rev.* B **44** 3802
[26] Northrup J E 1986 *Phys. Rev. Lett.* **57** 154
[27] Jung T 1996 private communication